Ocean Engineering 243 (2022) 110194

Contents lists available at ScienceDirect

Ocean Engineering

journal homepage: www.elsevier.com/locate/oceaneng

Seismic dynamics of a pipeline shallowly buried in loosely deposited seabed foundation

Jianhong Ye [a,*], Qianyu Lu [a,b]

[a] State Key Laboratory of Geomechanics and Geotechnical Engineering, Institute of Rock and Soil Mechanics, Chinese Academy of Sciences, Wuhan 430071, China
[b] University of Chinese Academy of Sciences, Beijing 100049, China

ARTICLE INFO

Keywords:
Pore pressure accumulation
Residual liquefaction
Loose seabed floor
Seismic wave
Submarine pipeline
Pastor–Zienkiewicz Mark III
FSSI-CAS 2D

ABSTRACT

It is widely known that submarine pipelines constructed in high seismic intensity zones are vulnerable due to soil liquefaction under the attack of seismic waves. It is meaningful for engineers to get insight into the seismic dynamic response mechanism of submarine pipelines, which mostly are buried in loosely deposited seabed floors in practical engineering. In this study, taking the integrated numerical model FSSI-CAS 2D as the platform, the seismic dynamic response of a shallowly buried submarine pipeline in a loosely deposited seabed floor is investigated. It is indicated by the numerical results that a shallowly buried submarine pipeline in loose seabed floor intensively responds to input seismic wave. Considerable vibration in horizontal and floatation in vertical occur for the pipeline due to the soil softening in the surrounding soil, as well as the soil liquefaction in the zone away from the pipeline. The buoyancy applied on the outer wall of the pipeline caused by the pore pressure accumulation makes a significant contribution to the upward floatation of the pipeline. It is found that the seismic wave-induced residual liquefaction firstly initiates in the medium depth of seabed floor due to the relatively great permeability of the loose seabed soil, and then develops toward to the upper and lower seabed synchronously. Because of the intensive interaction between the pipeline and its surrounding seabed soil, liquefaction has not occurred in the zone at the right and left-hand side of, as well as over the pipeline. Based on comparative analysis, it is found the magnitude of pipeline floatation if natural gas is transported is much greater than that if crude oil is transported. Finally, it is observed that considerable subsidence at the magnitude order of 1 m occurs for the pipeline in the post-reconsolidation process after seismic wave attacking. It is indicated by the analysis presented in this study that the integrated model FSSI-CAS 2D would be a trustworthy platform to study the seismic dynamic response of marine structures.

1. Introduction

Submarine pipeline is a kind of critical infrastructure in the offshore oil/gas industry, widely used in the offshore zone for the oil/gas transportation. Currently, there would be several hundred of thousands kilometres of submarine pipelines that have been installed in the world. Among them, the longest one is the Langeled pipeline engineering from Norway to the UK with a length of 1200 km. The stability of submarine pipelines is crucial for their normal service performance in their designed service period. However, submarine pipelines could easily lose their stability under the attack of ocean waves or seismic waves due to the breaking or buckling caused by the liquefaction of seabed soil. Some such kinds of catastrophic failures have been reported in the past decades, e.g. Christian et al. (1974), and Herbich et al. (1984). Therefore, it is meaningful for engineers to get insight into the dynamic characteristics of submarine pipelines under ocean wave loading or seismic wave attacking.

Generally, the instability of submarine pipelines could be attributed to scouring, ocean wave acting, or seismic wave attacking. On the scouring of seabed floor close to submarine pipelines, some valuable works have been conducted to understand the scouring mechanism under wave and current (Larsen et al., 2016; Kiziloz et al., 2013; Bayraktar et al., 2016; Fredsøe, 2016). However, scouring is not the focus of this study. On the wave-induced dynamics of marine pipeline and its seabed foundation, a few works have been conducted in the past two decades. Most of them were limited to the very dense seabed soil whose behaviour can be nearly modelled by poro-elastic model (Gao and Wu, 2006; Luan et al., 2008; Duan et al., 2017; Zhou et al., 2015; Zhang et al., 2011). In fact, there is another type of seafloor soil widely distributed in the offshore zone worldwide. It is the loosely deposited seabed soil, in which residual pore pressure could significantly be

* Corresponding author.
E-mail addresses: Jhye@whrsm.ac.cn, Yejianhongcas@gmail.com (J. Ye).

https://doi.org/10.1016/j.oceaneng.2021.110194
Received 9 April 2021; Received in revised form 10 November 2021; Accepted 11 November 2021
Available online 6 December 2021

accumulated under cyclic load, causing seabed soil to become liquefied (Summer et al., 2006). There were only a few works that have been conducted to study the wave-induced dynamics of submarine pipeline buried in loosely deposited seabed floor in the past two decades (Zhao et al., 2018; Dunn et al., 2006; Zhang et al., 2011; Ye and He, 2021). The latest brief literature view on the wave-induced dynamics of a pipeline is also available in Zhang et al. (2019) and Ye and He (2021).

About the seismic dynamic response of submarine pipelines shallowly buried in seabed floor, only little attention actually has been paid on this topic by scientists and engineers in the past. There are only few works that have been previously conducted in the past two decades. To the authors' best knowledge, there was no research work with substantial significance on this topic before 2000. After 2000, there were several works were performed to study the seismic dynamic response of loose seabed soil in which submarine pipeline was buried, e.g. Ling et al. (2008), Luan et al. (2009), Zhang and Han (2013) and Saeedzadeh and Hataf (2011). However, the effective stresses in loose seabed floor, and the seismic dynamic response of pipeline itself basically were not illustrated in these previous works. As a result, the insights on the seismic dynamic response characteristics and the instability mechanism of submarine pipelines buried in loose seabed floor is not comprehensive so far.

It is known that seismic wave is a type of crucial and non-ignorable environmental load for marine structures, such as the submarine pipelines involved in this study. It brings a great threat to the stability of offshore structures built on or shallowly buried in the loosely deposited seabed foundation. In this study, taking the integrated numerical model FSSI-CAS 2D as the platform, the seismic wave-induced dynamic response of a submarine pipeline shallowly buried in a loose seabed floor is comprehensively investigated. The analysis presented in this study could further enhance the insights on the seismic dynamic response of submarine pipelines buried in loose seabed floor.

2. Numerical model and constitutive model

In the marine environment, the overlying seawater, seabed floor, and buried pipelines is a coupled system. There is intensive interaction between them during subjected to ocean waves or seismic waves. In this study, the integrated numerical model FSSI-CAS 2D developed by Ye et al. (2013b) is taken as the computational platform, to investigate the complicated interaction between a buried pipeline and its surrounding loose seabed soil under the attack of seismic waves. It has been validated by previous studies (Ye et al., 2013b, 2014, 2013a; Ye and Wang, 2015) that FSSI-CAS 2D is a reliable and excellent numerical model for the problem of ocean/seismic wave-induced dynamics of offshore structures in the field of offshore geotechnics. More detailed information about FSSI-CAS 2D is available in Ye et al. (2013b) and Jeng et al. (2013). For the sake of brevity, they are not repeatedly introduced here.

It has been widely recognized that an elastoplastic constitutive soil model must be used to describe the complicated and nonlinear behaviour of seabed soil if it is being in loose state. In this study, the generalized plastic soil model Pastor–Zienkiewicz Mark III (PZIII thereafter) is used to describe the complicated behaviours of the surrounding loose seabed soil of pipelines under the action of seismic waves. PZIII model was initially established by Zienkiewicz and Mroz (1984) based on the generalized plasticity theory. Currently, PZIII has been implanted into FSSI-CAS 2D through the source codes programmed in Fortran language learning from the experiences of Chan (1988). The detailed information about the PZIII model can be found in Zienkiewicz et al. (1999). Overall, the PZIII model is an excellent constitutive soil model for clays and sandy soils. Its reliability has been validated by a series of laboratory tests involving monotonic and cyclic load, especially the centrifuge tests in the VELACS project. This model is one of the heritage of Olek Zienkiewics (Pastor et al., 2011).

It must be pointed out that the void ratio e and the related Darcy's permeability k should be variable depending on the volumetric deformation of the surrounding seabed soil of pipelines. In the case of seismic wave is applied, the effect of variable e and k on the dynamics of pipeline and its surrounding loose soil may be very significant. Therefore, the variation of e of seabed soil is taken into consideration following $e_{n+1} = (1 + e_n)\exp(\frac{\Delta p}{Q} + \Delta\epsilon_{vs}) - 1$, where n stands for nth time step in FE analysis, Δp is the incremental pore pressure, $\Delta\epsilon_{vs}$ is the incremental volumetric strain of soil, and Q is the compressibility of pore water. Correspondingly, the permeability of seabed soil k variates following $k = C_f \frac{e^3}{1+e}$, where C_f is an material coefficient, which can be estimated by $C_f = k_0 \frac{1+e_0}{e_0^3}$ (Miyamoto et al., 2004), where e_0 is the initial void ratio, and k_0 is the corresponding initial permeability.

3. Computational domain, boundary conditions and soil parameters

As demonstrated in Fig. 1, a steel pipeline (specific gravity at empty (SG) = 1.113) transporting crude oil with a wall thickness of 3 cm, and with an outer diameter of 800 mm is buried in the loosely deposited seabed floor in the offshore zone. The overlying water depth d is 10 m. The buried depth of the pipeline centre is 1.0 m. The computational domain of the loose seabed floor is 200 m long and 20 m thick. The pipeline is installed on the symmetrical line $x = 100$ m.

The bottom of the seabed floor is fixed both in x and z. On the upper surface, the hydrostatic pressure is applied following $P(x,t) = \rho_f g(d+s(x,t))$, where $s(x,t)$ is the subsidence of the surface of the seabed floor induced by seismic waves. If significant subsidence has occurred on the surface of the seabed floor, then its effect on the hydrostatic pressure on the seabed floor must be considered. Besides, the effective stresses on the upper surface of the seabed floor always keep zero because the seabed floor is permeable. Laminar boundary condition is applied to the two lateral boundaries. It means that there will be no seismic wave reflection on the lateral boundaries because they own the same displacements at their corresponding positions at any time.

To nearly simulate the working status of the pipeline, like that in Zhang et al. (2019), a pressure with 200 kPa driving oil/gas moving in the pipeline is applied to the oil/gas, and to the inwall of the pipeline. In reality, the horizontal and/or vertical movement of the surface of the seabed floor induced by seismic waves will of course lead to the motion of the overlying seawater through the interaction mechanism of the displacement continuity at the interfaces between the seawater and the seabed floor. As a result, tiny waves would be generated in the overlying seawater, and hydrodynamic load would be generated correspondingly. However, this hydrodynamic load cannot be estimated in this study, and certainly also cannot be considered in computation, because the integrated model FSSI-CAS 2D is just a one-way coupling model. Only water pressure is continuous at interfaces; while the displacement continuity at interfaces cannot be guaranteed in FSSI-CAS 2D. It means that the vibration of offshore structure and its seabed foundation cannot be fed back to influence the motion of seawater in FSSI-CAS 2D. If the seismic wave-induced hydrodynamic load on the seabed floor needs to be considered, then a fully coupled numerical model is needed. Unfortunately, such a fully coupled model is not yet available, so far as we know. As a consequence, only the hydrostatic water pressure is considered in the analysis.

The FE mesh of the pipeline-seabed floor system generated for computation is illustrated in Fig. 2. Totally 23316 quadrilateral elements (4-nodes) are generated. In the zone around the pipeline, the sizes of elements are in the range of 0.02–0.2 m, which are much smaller than that (0.5–2.0 m) in the other zone. In the mesh system, the pipeline is treated as an impermeable and rigid steel circle (its thickness is 3 cm), and the transported oil or gas in it is also discretized. A series of common nodes are used on the interface between the pipeline and its surrounding seabed soil because the contact problem involved in structure–soil interaction still cannot be handled by FSSI-CAS 2D so far. Because the pipeline is fully buried in this study, It results in that the surrounding seabed soil would not be out of contact with the pipeline

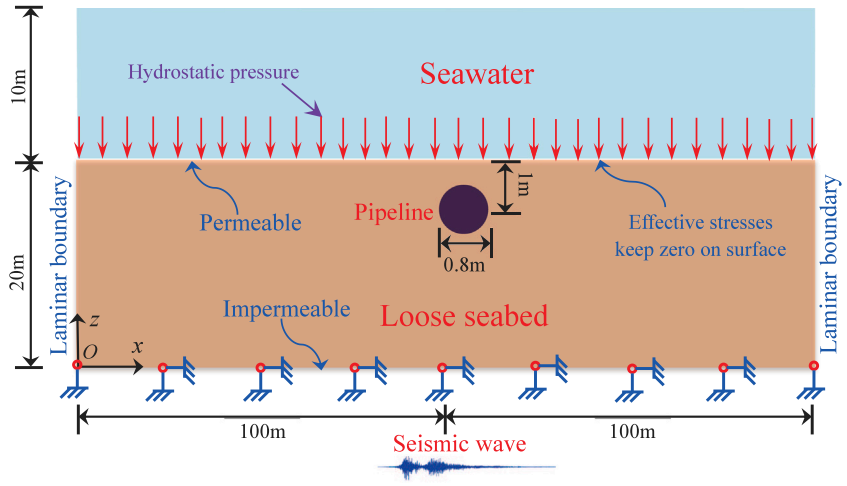

Fig. 1. Schematic diagram of the pipeline-seabed-seawater system used in computation.

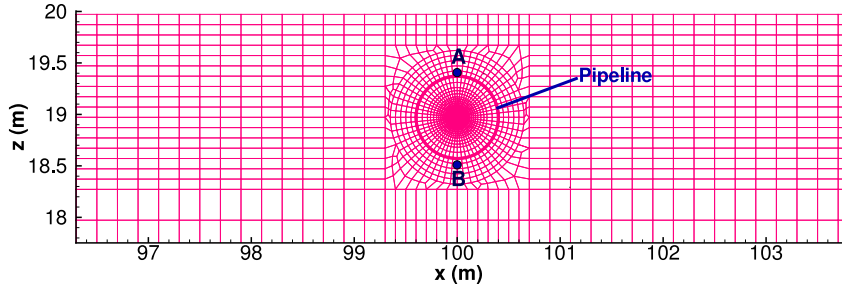

Fig. 2. Finite element mesh of the pipeline-seabed system in computation (Noted: the crude oil transported in the pipeline is also discretized, and only the mesh near to the pipeline is shown here. A (x = 100 m, z = 19.45 m), B (x = 100 m, z = 18.55 m) are two typical points to demonstrate the computational results).

during seismic events. Even so, the relative slipping at the peripheral direction between the pipeline and its surrounding seabed soil would be significant. However, this peripheral relative slipping also cannot be handled so far by FSSI-CAS 2D, as mentioned above. The influence of this contact effect between the pipeline and its surrounding seabed soil on the seismic dynamic response could be further investigated in the future. Two typical points A (x = 100 m, z = 19.45 m), B (x = 100 m, z = 18.55 m) over and beneath the pipeline labelled in Fig. 2, and another typical point E (x = 100 m, z = 15 m) beneath the pipeline are chosen to demonstrate the seismic dynamic response characteristics of the surrounding loose seabed soil of the pipeline in the subsequent sections.

Parameters of the loosely deposited seabed soil for the constitutive model PZIII are listed in Table 1. They were calibrated by Zienkiewicz et al. (1999) for Nevada sand with a relative density D_r = 60% when taking part in the VELACS project. In fact, those model parameters for PZIII can be calibrated by performing a number of laboratory tests for real seabed soils. The initial void ratio e_0, saturation S_r of the seabed soil used in the analysis is 0.7372, and 98%, respectively. Correspondingly, the initial permeability is estimated as 7.2×10^{-5} m/s.

Table 1
Model parameters of loose seabed soil for PZIII in analysis.

Iterm	Note	Value	Unit
K_{evo}	Bulk modulus	2000	[kPa]
G_{eso}	3× Shear modulus	2600	[kPa]
p'_0	Confining pressure for K_{evo}, G_{eso}	4	[kPa]
M_g	Slope of CSL	1.32	–
M_f	Slope of phase transformation line	1.3	–
α_f	Material parameter	0.45	–
α_g	Material parameter	0.45	–
β_0	Material parameter	4.2	–
β_1	Material parameter	0.2	–
H_0	Material parameter	750	–
H_{U0}	Material parameter	40,000	–
γ_u	Material parameter	2.0	–
γ_{DM}	Material parameter	4.0	–

4. Input seismic wave

Comparing with a synthetic seismic wave, a seismic wave truly recorded in offshore area would be the best choice to be the input seismic excitation in seismic analysis. In this study, the recorded seismic wave, as illustrated in Fig. 3, recorded in the Japan 311 off-Pacific coast of Tohoku earthquake (M_L = 9.0) at the observation station MYGH03 (141.6412E, 38.9178N, buried depth = 120 m, at Karakuwa, Japan), which is near to the Pacific coastal line, is taken as the input seismic wave. The horizontal (E-W) and vertical (U-D) components of this seismic acceleration wave are applied to the bottom of the seabed floor synchronously in computation. It should be noted that the computational case presented in this study is only a 2D analysis under the condition of plane strain, because the pipeline is a type of linear structure. The seismic wave-induced surface waves in the superficial layer of seabed, e.g. Love wave and Rayleigh wave, cannot be considered in this 2D analysis.

5. Results analysis

Because of that, the seismic dynamic response of loose seabed floor without buried pipeline has been comprehensively demonstrated in Ye and Wang (2016), it is only necessary to analyse the seismic dynamic response of the buried pipeline and its surrounding loose seabed soil in this study.

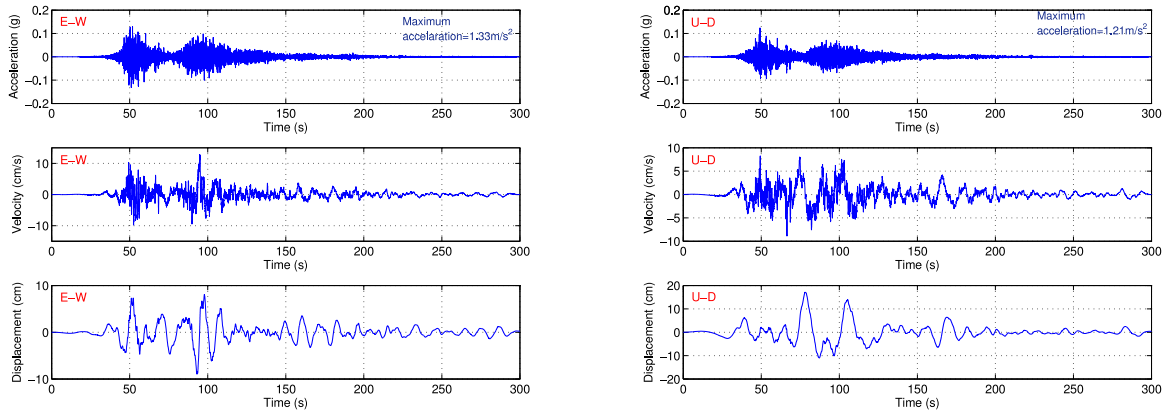

(a) Horizontal (E-W) (b) Vertical (U-D)

Fig. 3. Input seismic wave after wave filtering adopting the recorded seismic wave at the station MYGH03 at Karakuwa, Japan during 311 off-Pacific earthquake event. Noted: noncausal butterworth filter is used; filtering range: $f \leq 0.03$ Hz and $f \geq 30$ Hz.

5.1. Initial status

Before the input seismic wave arriving at, there should be an initial state for the pipeline-seabed floor system. This initial state should be taken as the initial condition for the subsequent seismic analysis. A detailed analysis on the initial displacement, pore pressure, and effective stresses of the seabed-pipeline system is available in Zhang et al. (2019). Overall, the pipeline has a significant effect on the initial distribution of displacement, and effective stresses in the surrounding seabed soil of the pipeline.

5.2. Seismic dynamics of pipeline

The time history of the acceleration of the buried pipeline responding to the input seismic wave is illustrated in Fig. 4. It is observed that the peak horizontal acceleration of the pipeline is only 0.042 g, which is much less than that (0.136 g) of the input seismic wave. Another obvious characteristic is that there is basically no horizontal acceleration response, while there is still the vertical acceleration response for the pipeline after $t = 60$s. If looking into the input horizontal acceleration, as illustrated in Fig. 3, it is found there is always a horizontal component in the input seismic wave after $t = 60$s. What is the reason for the phenomenon that the horizontal responding acceleration of the pipeline basically disappears after $t = 60$s? It is indicated by the subsequent analysis in this study that the seismic wave-induced residual liquefaction in the loose seabed floor is the efficient cause for this phenomenon. It is well known that a loosely deposited seabed soil is highly prone to become liquefied under cyclic loads, such as ocean waves and seismic waves. This recognition has been proved once and once again in several previous studies (Sassa and Sekiguchi, 2001; Ye and Wang, 2016; Miyamoto et al., 2020; Yang and Ye, 2017; Teh et al., 2003; Yang and Ye, 2018; Summer et al., 2006; Ecemis et al., 2021). Once the residual liquefaction occurs in a loose seabed floor, it will behave like a type of heavy fluid with a great viscosity. It is also well known in physics that shear waves cannot be transmitted in fluidized materials, but the longitudinal waves can be. In this study, the horizontal component of the input seismic wave is similar to a shear wave, while the vertical component is similar to a longitudinal wave for the seabed floor. Even though the residual liquefaction has occurred, the vertical component of the input seismic wave can be still transmitted in the liquefied seabed floor. That is the reason why there is still vertical responding acceleration for the pipeline after $t = 60$s. Besides, the peak vertical acceleration of the pipeline is 0.202 g, which is significantly greater than that of the input seismic wave.

Response spectrum can be used to identify the amplification effect to the input seismic wave. Fig. 5 shows the acceleration spectrum of the pipeline. It can be seen in Fig. 5 that basically all frequency components in the horizontal input seismic wave (E-W) are damped by the pipeline-loose seabed floor system. However, for the vertical input seismic wave (U-D), the high-frequency components ($f > 1$ Hz) are amplified; and the low-frequency components ($f < 0.5$ Hz) are damped by the pipeline-loose seabed floor system. For the frequency components from 0.5 Hz to 1 Hz in the vertical input seismic wave (U-D), the damping or amplification effect is not significant. This characteristic of the acceleration response spectrum of the buried pipeline certainly have a closed relationship with the occurrence of residual liquefaction in the loose seabed floor, as analysed above. Overall, the seismic wave-induced residual liquefaction is the main controlling factor for the seismic dynamic response of the buried pipeline. This will be clearly reflected in the following analysis on the pore pressure accumulation and on the development of residual liquefaction zone.

The time history of the displacements of the buried pipeline is shown in Fig. 6. It is observed that there is intensive vibration in horizontal for the buried pipeline. Before $t = 60$ s (Noted: this time is a critical time for the residual liquefaction occurrence in the loose seabed floor), there are a great number of high-frequency oscillations in the time history of the horizontal displacement. After $t = 60$ s, there are only a series of low-frequency horizontal vibrations with great amplitude. The reason is that these high-frequency components in the horizontal input seismic wave have been filtered by the liquefied and fluidized seabed soil after $t = 60$ s. After the occurrence of liquefaction in the loose seabed floor, the response of the buried pipeline is much more intensive than that before $t = 60$ s. The peak horizontal amplitude of the pipeline reaches up to 18 cm. Besides, the resonance phenomenon in horizontal can be clearly observed in the later stage. At the end of the seismic wave attacking, the horizontal residual displacement is about 3 cm toward to the $+x$ direction.

In the time history of the vertical displacement of the pipeline, it is interesting to find that the pipeline firstly sinks about 6.5 cm before $t = 60$ s, and then continuously floats up about 4 cm under the attack of seismic wave. Finally, the pipeline only subsides about 2.5 cm relative to its initial position in the initial state. This type of motion mode of the pipeline is closely related to the accumulation process of pore pressure in the surrounding loose seabed soil of the pipeline under cyclic loads. As mentioned above, it has been widely known that the pore pressure will build up in loose seabed floor under cyclic loads, regardless of from the perspective of numerical modelling or laboratory tests (Sassa and Sekiguchi, 2001; Ye and Wang, 2016; Miyamoto et al., 2020; Yang and Ye, 2017; Summer et al., 2006; Ecemis et al., 2021).

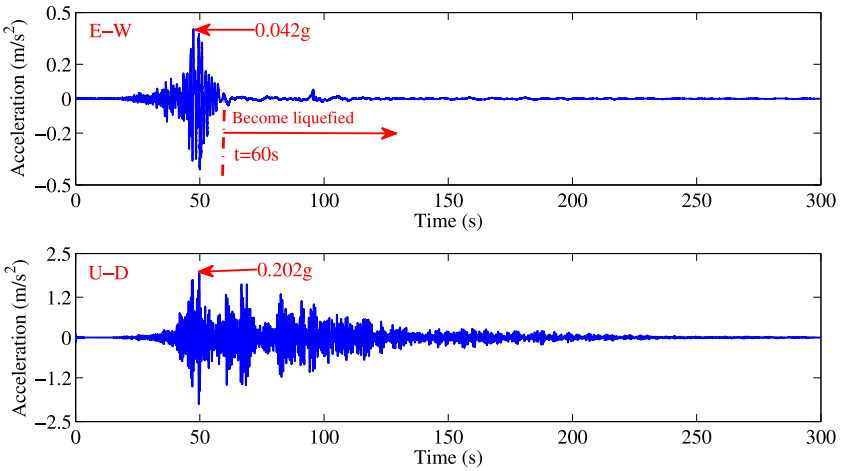

Fig. 4. Time history of the acceleration of the pipeline responding to the input seismic wave.

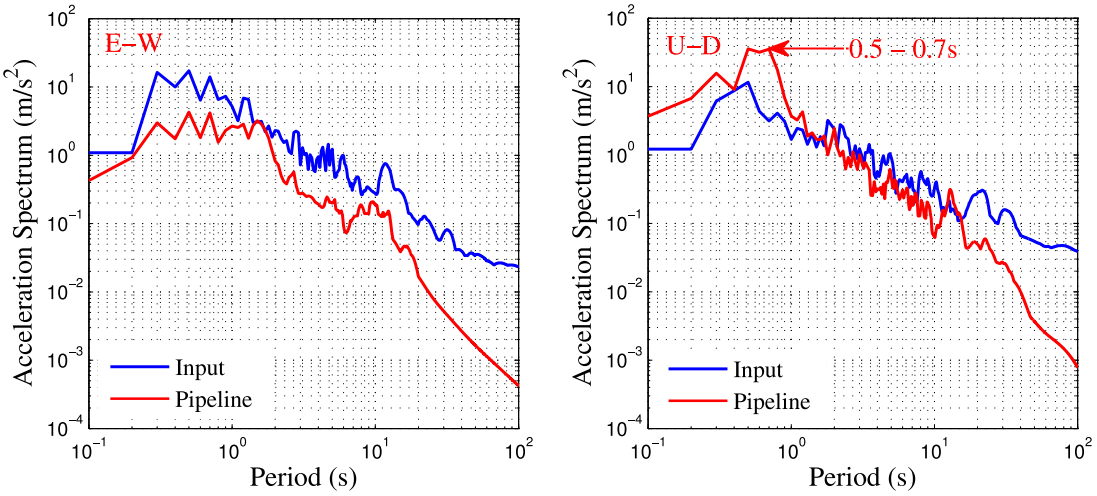

Fig. 5. Acceleration response spectrum of the pipeline.

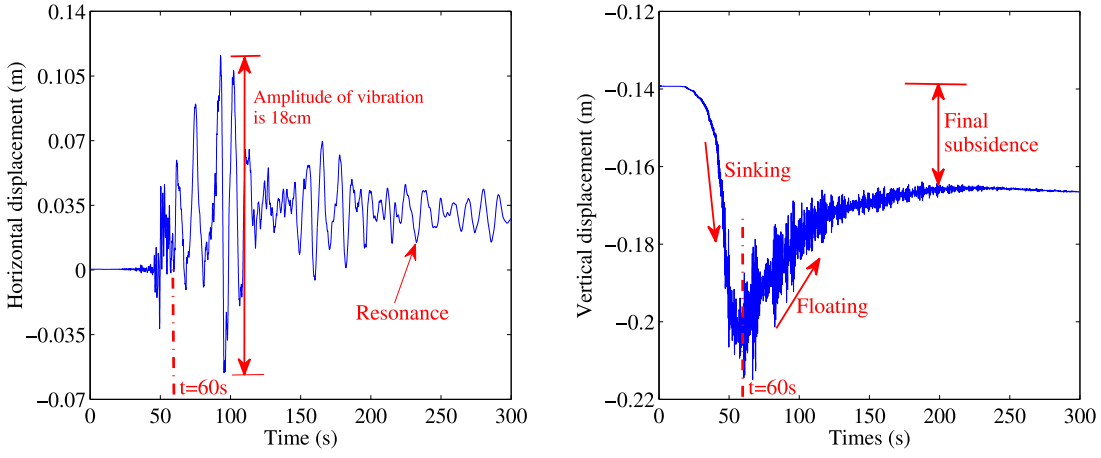

Fig. 6. Time history of the displacements of the pipeline induced by the seismic wave (Noted: the initial subsidence in the initial state is not excluded).

Accompanying the pore pressure accumulation in the surrounding soil, the buoyancy applied on the buried pipeline becomes greater and greater, as demonstrated in Fig. 7. At the early stage, the buoyancy is less than the gravity of the pipeline-oil system. Correspondingly, the pipeline subsides firstly. After the buoyancy on the pipeline becoming greater than the gravity of the pipeline-oil system, the sinking of the pipeline gradually is inhibited, and finally the floatation occurs for the pipeline under the continuous help of the considerable buoyancy generated by the excess pore pressure. It should be noted that the time (about t = 60 s) when the vertical motion of the pipeline switching from sinking to floating is not the same as that (about t = 50 s) when the buoyancy is equal to the gravity of the pipeline-oil system. It is

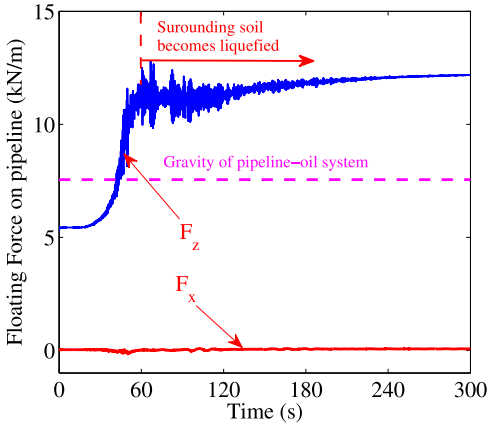

Fig. 7. Development of the buoyancy applied on the pipeline induced by the pore pressure accumulation in the surrounding soil.

indicated that the interaction between the pipeline and its surrounding loose seabed soil under the seismic wave is complicated and nonlinear. We cannot understand their interaction adopting a linear thinking, because the pipeline did not immediately float up once the buoyancy is equal to the gravity of the pipeline-oil system. Finally, it is observed in Fig. 7 that the buoyancy has not infinitely grown up under seismic wave attacking. This is because the residual pore pressure will not easily further grow up at a position where residual liquefaction once occurs in loose seabed floor, unless an extra load is transferred to this position due to the shift of gravity centre of marine structures, or due to the large deformation of seabed foundation, as analysed in Ye and Wang (2015). So far as we have known, this is the first time that the sinking and floatation of a buried pipeline under seismic loading are finely captured by numerical modelling in the field of offshore geotechnics. It is indicated that FSSI-CAS 2D is an excellent numerical model to characterize the interaction between marine structure and its seabed foundation under the attack of seismic waves.

Due to the unique motion mode of the pipeline in vertical (sinking first, and then floating up), the seabed soil overlying the pipeline upheaves caused by the upward extrusion of the floating pipeline, as illustrated in Fig. 8. There is an obvious upheaval zone over the buried pipeline. In the zone away from the pipeline, the seabed soil significantly subsides relative to the surrounding soil of the pipeline. It is indicated that the pipeline has a significant effect on the dynamics of its surrounding seabed soil.

5.3. *Effective stresses and pore pressure in seabed foundation*

The time histories of the pore pressure, effective stress I_1 and void ratio e at the two typical positions A ($x = 100$ m, $z = 19.45$ m) and B ($x = 100$ m, $z = 18.55$ m) in the surrounding soil of the pipeline are shown in Fig. 9. It is found that the variation processes of the pore pressure, effective stress I_1 and void ratio e at A and B are highly similar. However, there are also several differences presented in these variation processes, since A and B are located at different orientations of the buried pipeline. The overall variation process is that the residual pore pressure builds up quickly first to its peak value, and then gradually is dissipated or basically remains unchanged under the seismic wave attacking. Correspondingly, the effective stress in the surrounding soil reduces first (Noted: negative means compressive), and then grows in this process. It is worthy to be noticed that the effective stress I_1 at A and B has never arrived at the zero-stress state (fully liquefied). It is indicated that it is impossible for the surrounding soil at A and B to become fully liquefied state under the seismic wave attacking. Only partial liquefaction could be possible at A and B. The void ratio e at A is always reduced, indicating that the soil at A is contractive all the time, and becomes denser and denser. However, the soil at B is contractive before $t = 105$ s, and then is dilative caused by the upward floatation of the pipeline. Because A, B is respectively located above and beneath the pipeline, the floatation of the pipeline will certainly extrude the soil at A, and drag the soil at B.

In Fig. 9, it is also observed that the residual pore pressure at A gradually reduces in the later stage of the seismic wave attacking. It is mainly attributed to the facts: (1) The soil at A gradually upheaves caused by the floatation of the pipeline, making the distance from A to the static water level reduced. This mechanism certainly causes the pore pressure at A reduced. (2) The drainage path from A to the surface of the seabed floor is relatively short, making the pore pressure at A is easily dissipated accompanying the drainage of pore water. For the soil at B beneath the pipeline, its upheaval is not significant, as shown in Fig. 8; and the drainage of pore water is blocked by the steel pipeline. As a result, the residual pore pressure at B can basically remain unchanged in the later stage of the seismic wave attacking. Another interesting phenomenon observed in Fig. 9 is that the effective stress I_1 at B significantly grows in the period from about $t = 60$ s to 120 s, while the residual pore pressure at B basically remains unchanged, as illustrated above. It seems that this phenomenon is contradictive with the previous conventional recognition which thinks that the growth of effective stress should be accompanied by the reduction of residual pore pressure. Otherwise, the typical effective stress principle $\sigma_{ij} = \sigma'_{ij} + \delta_{ij} p$ may not hold. Actually, this phenomenon can be attributed to the complicated interaction between marine structures and its seabed foundation. An extra load has been transferred from other locations to B in the interaction process. If the soil at B is not fully liquefied, then the extra load must be all beard by the soil skeleton. As a consequence, the effective stress at B grows, while the residual pore pressure at B can remain unchanged. If the soil at B has become fully liquefied behaving like a type of fluidized material (effective stress is zero), then the extra load must be all beard by the pore water. As a consequence, the pore pressure at B will grow significantly, while the effective stress at B will still keep as zero. This interaction mechanism also has been analysed in Ye and Wang (2015), He et al. (2018). Overall, this type of phenomenon is quite common in the cases involving the interaction between marine structure and its loose seabed foundation under ocean wave or seismic wave attacking. If a numerical model cannot capture this type of phenomenon in simulation, then this numerical model is not reliable to a certain extend. Therefore, the reliability of a numerical model could be verified by that whether the above described nonlinear interaction phenomenon can be captured or not, in our opinion.

The typical position E is also under the pipeline with a distance of 4 m to the pipeline centre. The time histories of pore pressure, I_1 and the void ratio at E are demonstrated in Fig. 10. Due to the fact that E is away from the pipeline, the effect of the pipeline on the dynamics of soil at E basically disappears. Therefore, the variation processes of pore pressure, effective stress, and void ratio at E are relatively simple compared with that at A and B. The dynamics of soil at E is highly similar to that previously illustrated in Ye and Wang (2016). Under the seismic wave attacking, the pore pressure at E quickly builds up until to $t = 60$ s. After that, the residual pore pressure basically remains unchanged. However, the oscillatory pore pressure is significant in this stage. The effective stress I_1 correspondingly significantly reduces. After $t = 60$ s, the loose seabed soil at E becomes partially liquefied because I_1 is not zero at this moment. The soil at E becomes fully liquefied about at $t = 110$ s. After this moment, the soil at E always keeps the fully liquefied state. Due to the slight effect of the pipeline, the shear stress at E is not zero at initial. Before $t = 60$ s, there is a significant shear stress wave transmitted by the soil at E. However, once partial liquefaction occurs at E, the magnitude of the shear stress immediately significantly reduces. After $t = 110$ s, there is no shear stress at E because shear waves cannot be transmitted by fully liquefied soil. The void ratio at E is always contractive in the whole process, indicating that the soil at E gradually becomes denser and denser accompanying the drainage

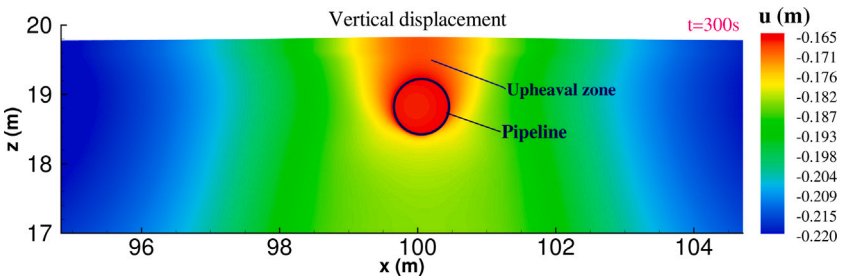

Fig. 8. Distribution of the vertical displacement in the loose seabed foundation at the end of the input seismic wave (Noted: the initial subsidence in the initial state is not excluded).

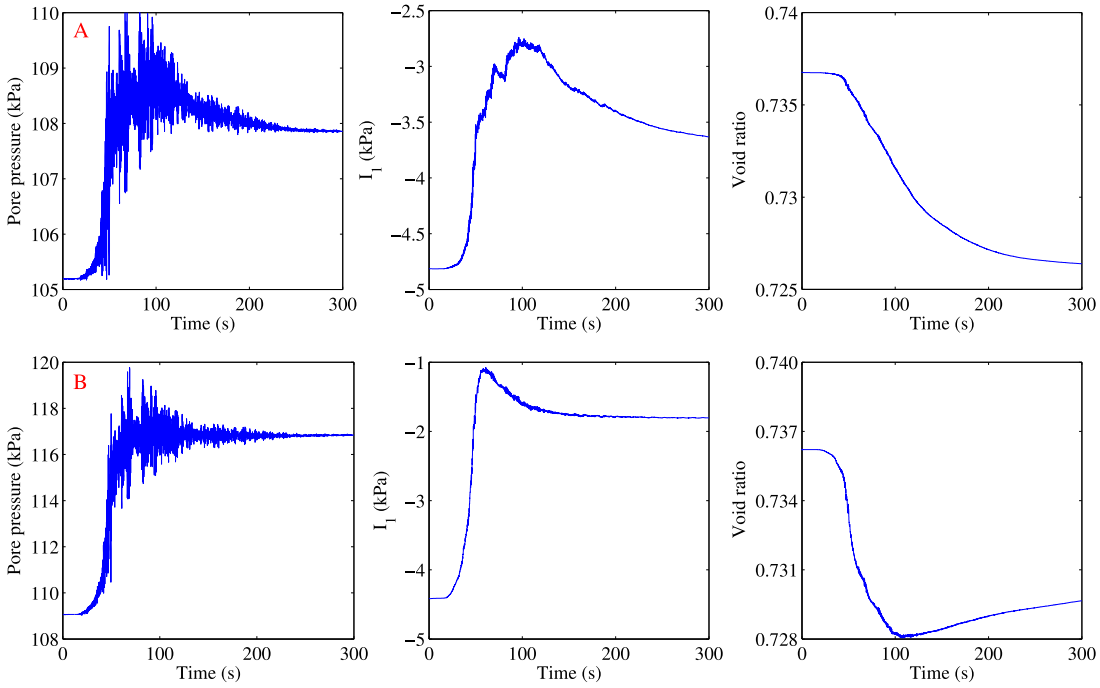

Fig. 9. Time history of pore pressure, I_1 and void ratio at the typical position A (x = 100 m, z = 19.45 m) and B (x = 100 m, z = 18.55 m) in the surrounding soil (Noted: negative means compressive).

process of pore water from seabed floor to overlying seawater under the attack of the seismic wave. This mechanism actually also has been clearly analysed by Ye and Wang (2016) for a flat seabed floor without any marine structures. Overall, the dynamics of the soil away from the pipeline is significantly different from that of the surrounding soil of the pipeline.

Besides, the distribution of the residual pore pressure and I_1 around the pipeline in the surrounding soil at several typical times are shown in Fig. 11. It is clearly found that the accumulation of pore pressure is not uniform. The accumulation rate in the surrounding soil under the pipeline is faster than that over the pipeline. Furthermore, the distribution of residual pore pressure is symmetric along x = 100 m at any moment. Correspondingly, the reduction of effective stress $-I_1$ under the pipeline is faster than that over the pipeline. There is also basic symmetry for the distribution of I_1 around the pipeline at any moment.

5.4. Liquefaction

It has been widely recognized that there are two types of liquefaction mechanisms for seabed soil. They are momentary liquefaction and residual liquefaction. Momentary liquefaction generally can only occur in very dense seabed soil in the zones under wave troughs. Residual liquefaction is always prone to occur in loose seabed floors caused by the pore pressure accumulation under ocean waves or seismic waves attacking. Once residual liquefaction occurs in seabed foundation, it would bring a great threat to the stability of marine structures built on the seabed foundation, as demonstrated in Ye and Wang (2015). For the pipeline involved in this study, it is buried in the seabed floor, rather than is laid on the seabed floor. So far as we know, there are few works have been conducted to study the effect of residual liquefaction on the stability of a pipeline buried in loosely deposited seabed floor. In this section, the development of the residual liquefaction zone in the surrounding soil of the buried pipeline will be investigated.

Generally, there are two kinds of criteria adopted to quantitatively evaluate and judge the occurrence of residual liquefaction (Yang and Ye, 2018). They are the pore pressure-based criterion and stress-based criterion. For the pore pressure-based criterion, a ratio $r_u = \frac{p_{excess}}{-\sigma'_{z0}}$ between the excess pore pressure p_{excess} and the initial effective stress σ'_{z0} is defined. If r_u is greater than a critical value, e.g. 0.8, residual liquefaction could be judged to occur for the soil at a position. Unfortunately, there is a congenital defect for this pore pressure-based criterion. As pointed out by Ye and Wang (2015), this type of criterion can only be used for the cases in which there is no offshore structure involved. If an offshore structure is built on or buried in a seabed floor, the pore pressure-based criterion is actually not a reliable criterion to judge the occurrence of residual liquefaction due to the fact that there probably is intensive soil–structure interaction. It has previously

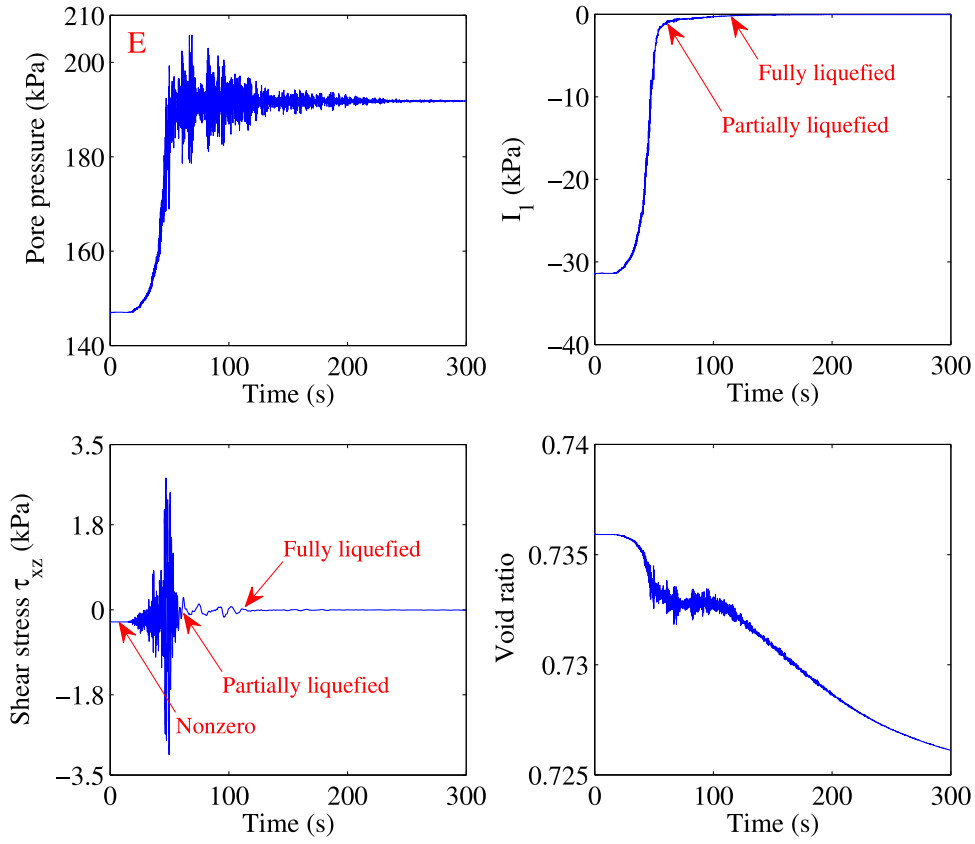

Fig. 10. Time history of pore pressure, $-I_1$ and void ratio at the typical position E which is far away from and beneath the pipeline.

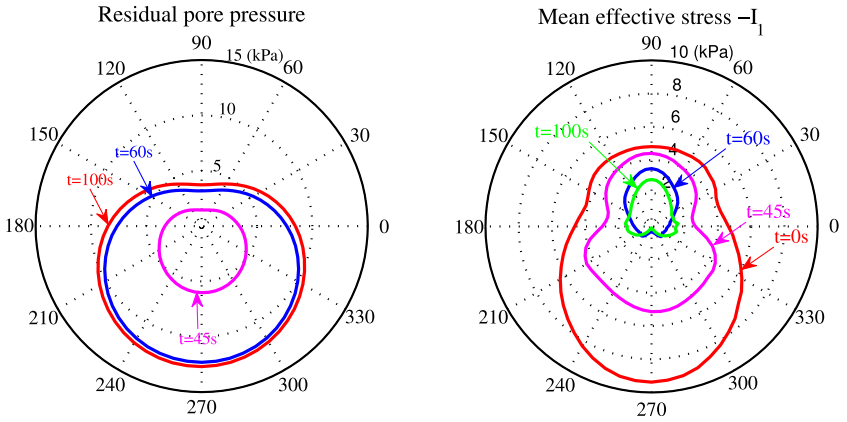

Fig. 11. Distribution of residual pore pressure and I_1 around the pipeline at several typical times.

been recognized that there would be load/stress transferring from one position to another position in seabed foundations in the process of soil–structure interaction. As a result, the phenomenon may occur that the residual pore pressure is much greater than the initial effective stress σ'_{z0} at a position, however, the current effective stress at this position is still far away from the zero-stress state. In this case, the soil at this position definitely could be judged to has been fully liquefied according to this pore pressure-based criterion, but the soil at this position actually is not liquefied. Therefore, the pore pressure-based criterion is invalid in this case. Summarily, the pore pressure-based criterion actually is an indirect judgement criterion. It is not suggested by Ye and Wang (2015) to be used in the cases where soil–structure interaction is involved.

The second method is based on the effective stress. According to the traditional definition of soil liquefaction, the most obvious physical characteristic of soil liquefaction is that the effective stress between soil particles approaches zero (partially liquefied) or exactly is equal to zero (fully liquefied). Therefore, we can adopt this physical characteristic to judge the occurrence of soil liquefaction. As a result, the effective stress-based criteria is a type of direct criteria. Based on this recognition, two specific formulations have been proposed by the first author in previous literature (Ye and Wang, 2015; Yang and Ye, 2018) to evaluate the residual liquefaction in loose seabed soil. The first one is that a parameter referred as to residual liquefaction potential $L_{\text{potential}}$ is defined to describe the liquefaction potential of seabed soil under cyclic loads (Noted: negative means compressive):

$$L_{\text{potential}} = \frac{\sigma'_{zd}}{-\sigma'_{z0} + \alpha c} \geq (L_p)_{\text{critical}} \tag{1}$$

where $\sigma'_{zd} = \sigma'_z - \sigma'_{z0}$ is dynamic vertical effective stress; σ'_{z0} is initial vertical effective stress; σ'_z is current vertical effective stress. c is the cohesion of seabed soil; α is a material coefficient, the discussion on α can be found in Ye and He (2021). In this study, cohesion c is zero for Nevada sand. For sandy seabed soil, the residual liquefaction potential can be expressed as $L_{\text{potential}} = 1 - \frac{\sigma'_z}{\sigma'_{z0}}$. If the effective stresses in 3D situation are considered, it becomes $L_{\text{potential}} = 1 - \frac{I_1}{(I_1)_0}$, where $(I_1)_0$ is the initial mean effective stress. $(L_p)_{\text{critical}}$ is a critical value given by engineers and scientists. When $L_{\text{potential}}$ is greater than or equal to the given $(L_p)_{\text{critical}}$ at a position, the soil at this position can be judged to become liquefied. On the issue of the value range of $L_{\text{potential}}$, it is generally in the range of 0.0 to 1.0. In the case involving intensive soil–structure nonlinear interaction, $L_{\text{potential}}$ in some local zones could be less than 0.0 due to the fact that the current $|\sigma'_z|$ could be greater than $|\sigma'_{z0}|$, even though the pore pressure has been significantly built up at a position, as the results presented in Ye and Wang (2015). Fortunately, there is no effect on the reliability of $L_{\text{potential}}$ under this circumstance to judge the occurrence of residual liquefaction, because $L_{\text{potential}} < 0$ and the soil at this position indeed has not liquefied.

The second judgement formulation for the effective stress-based criteria is $|I_1| \leq (I_1)_{\text{critical}}$, where $(I_1)_{\text{critical}}$ is also a critical value given by engineers and scientists. It means that the residual liquefaction will occur at a position where the current mean effective stress $|I_1|$ is less than or equal to the given critical value $(I_1)_{\text{critical}}$. Due to the fact that sandy soil cannot bear any tensile stress, the mean effective stress I_1 in sandy seabed soil must be negative. Generally, the critical value $(I_1)_{\text{critical}}$ given by engineers and scientists is a small value close to zero, e.g. 1 kPa. In theory, the current $|I_1|$ must be very small in the partially liquefied situation or must be equal to zero in the fully liquefied situation. In theory, this effective stress-based judgement formulation in which the current $|I_1|$ is used is more in line with the definition of liquefaction than that of $L_{\text{potential}}$.

It should be noticed that the above two stress-based criteria neither is perfect. They each have their own strengths and weaknesses. For the first judgement formulation expressed by Eq. (1), the value of α currently is impossible to be quantitatively determined through laboratory tests or theoretic analysis. As a consequence, Eq. (1) is not applicable for clay and silty soil. Additionally, the critical value $(L_p)_{\text{critical}}$ is not a constant value for all types of soils, but need to be given by engineers or scientists based on their engineering experiences and theoretic analysis. As a result, an unexpected artificial error would be brought. According to the suggestion of Wu et al. (2004), $(L_p)_{\text{critical}}$ could be in the range of 0.78–0.99, depending on the soil types. In this study, $(L_p)_{\text{critical}} = 0.8$ will be used to predict the residual liquefaction zone in the loose seabed floor. For the second judgement formulation, the unexpected artificial error is also unavoidable when determining the critical value $(I_1)_{\text{critical}}$, for example, the size and shape of the predicted residual liquefaction zone would be significantly different when $(I_1)_{\text{critical}} = 1$ kPa or $(I_1)_{\text{critical}} = 2$ kPa. Another defect of the second judgement formulation is that it is not applicable to judge the liquefaction for the upper seabed soil with shallow buried depth, e.g., the absolute mean effective stress $|I_1|$ is certainly less than 1 kPa for the seabed soil with a buried depth less than 5 cm (near to seabed surface) at the initial state, as a result, the seabed soil will be wrongly judged to become liquefied all the time if $(I_1)_{\text{critical}} = 1$ kPa, even though there is no seismic wave has been applied to the seabed floor. However, the second judgement formulation has huge advantages to judge the occurrence of liquefaction for the seabed soil with a great initial effective stress, e.g. 100 kPa.

The predicted residual liquefaction zone in the seabed floor induced by the seismic wave adopting the two stress-based criteria are shown in Fig. 12. The corresponding distributions of the mean effective stress I_1, shear stress τ_{xz} and pore pressure at $t = 100$s are also shown in Fig. 13. It is found that the predicted liquefaction zones are significantly different adopting the two stress-based criteria. If the first criteria $|I_1| \leq (I_1)_{\text{critical}} = 1$ kPa is adopted, it is observed that the soil over the pipeline is not liquefied at all times caused by the upward extrusion of the floating pipeline. Liquefaction only occurs in the superficial layer of the seabed floor (Noted: this zone probably is misjudged due to the reason presented above), as well as in a narrow surrounding zone under the pipeline at $t = 60$ s. After 10 s, the liquefaction zone is quickly enlarged downward. However, there is a zone beneath the pipeline that is not liquefied. At $t = 100$ s, liquefaction further occurs in this zone under the pipeline.

If the second criteria $L_{\text{potential}} = 1 - \frac{\sigma'_z}{\sigma'_{z0}} \geq (L_p)_{\text{critical}}$ is adopted, it also can be observed that the soil over the pipeline is not liquefied at all time caused by the upward extrusion of the floating pipeline. At $t = 60$ s, the seabed superficial soil is not liquefied, while the soil under $z = 18.2$ m is liquefied. Furthermore, the soil beneath the pipeline is also liquefied, and it is connected to the liquefaction zone below. After 10 s, the frontier of the liquefaction zone has further developed upward to $z = 19$ m. At $t = 100$ s, the frontier of the liquefaction zone has arrived at the surface of the seabed floor in the zone away from the pipeline. However, the liquefaction zone no longer enlarges in the surrounding soil of the pipeline due to the intensive soil–structure interaction after $t = 60$ s.

Overall, it seems that the development process of the liquefaction zone predicted by the first stress-based criteria is more regular. In our opinion, we are more inclined to think that the predicated liquefaction zone taking by the first stress-based criteria is more reasonable. The reasons are that: (1) The second stress-based criteria naturally is not good at handling the liquefaction prediction for the soil with shallow buried depth. (2) The liquefaction zone predicted by the second stress-based criteria at $t = 70$ s looks a little odd, as shown in Fig. 12(a). (3) The distribution zone where the shear stress τ_{xz} is not zero around the pipeline at $t = 100$s, shown in Fig. 13, is basically overlapped with the liquefaction zone predicated by the first stress-based criteria. It is maybe implied that the second stress-based criteria $|I_1| \leq (I_1)_{\text{critical}}$ is not enough reliable for the case involved in this study.

It is indicated by previous studies (Ye and Wang, 2016; Sassa and Sekiguchi, 2001; Miyamoto et al., 2020; Yang and Ye, 2017) that the residual liquefaction generally firstly initiates at the surface of seabed floor, and then gradually enlarges downward under ocean wave or seismic wave loading. However, it has been predicted that the frontier of the residual liquefaction zone gradually develops upward, and finally arrives at the surface of the seabed floor if the first stress-based criterion is used, as demonstrated in Fig. 12(b). It seems that the computational results presented in this study are contradictive with the previous recognition. Here, the development process of the residual liquefaction in the loose seabed floor is further investigated.

The distribution of the liquefaction potential L_p along with the seabed depth on $x = 100$ m at several typical times are illustrated in Fig. 14. Like that in Fig. 12, $(L_p)_{critical}$ is also set as 0.8 here. It is found that the L_p on $x = 100$ m are all less than 0.8 before $t = 48$ s. Just after two seconds, L_p on $x = 100$ m in the depth from $z = 4$ m to $z = 16$ m becomes greater than 0.8. It means that the soil in the range from $z = 4$ m to $z = 16$ m all becomes liquefied in the period from $t = 48$ s to 50 s. It is also clearly observed that L_p on $x = 100$ m are all greater than 0.8 when $t \geq 55$ s. It is indicated that the seabed soil on $x = 100$ m has all become liquefied during $t = 50$ s to 55 s. Based on the development characteristics of liquefaction on $x = 100$ m, it is recognized that the liquefaction should initiate in the medium depth, and then enlarge toward into the upper and lower depth of the seabed floor synchronously. This phenomenon is significantly different from the previous recognition, as that demonstrated in Ye and Wang (2016), which claimed that the seismic wave-induced residual liquefaction should initiate at the upper seabed, and then enlarge downward. Through comparative analysis, it is known that the different development mode of the liquefaction zone is caused by the permeability of seabed soil. In Ye and Wang (2016), the initial permeability of seabed soil is set as 1.0×10^{-5} m/s; while it is 7.2×10^{-5} m/s in this study, which is 7.2 times of that set

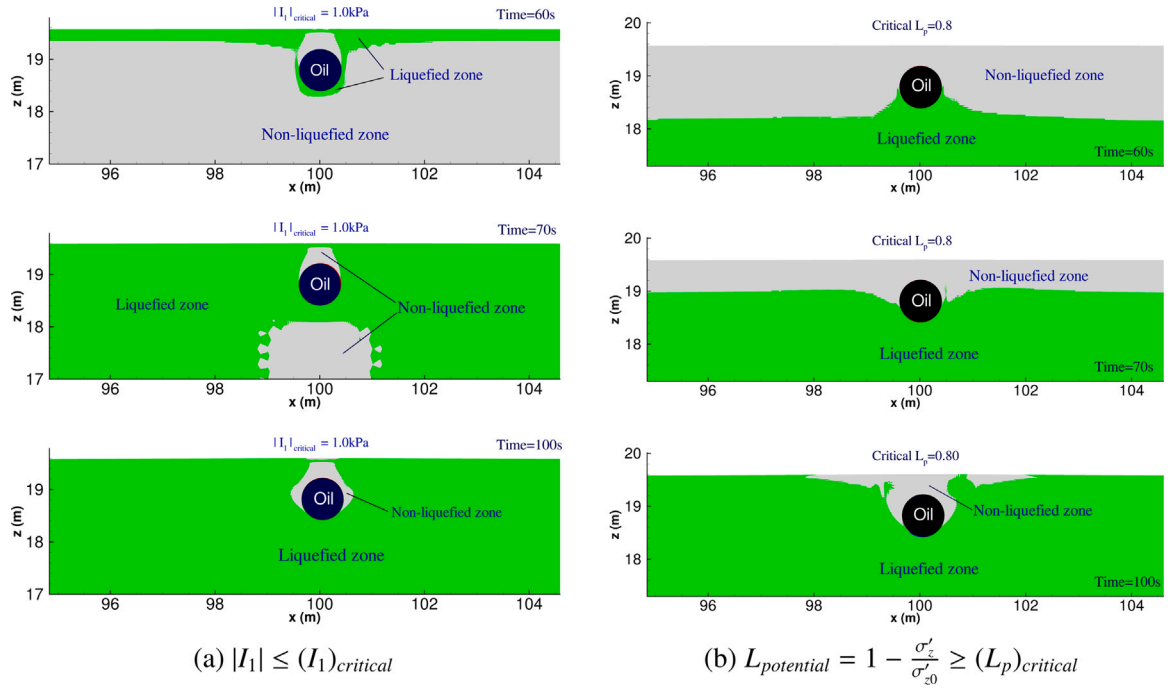

Fig. 12. Predicted liquefaction zone in the loose seabed floor at three typical times induced by the seismic wave adopting the two stress-based criterion.

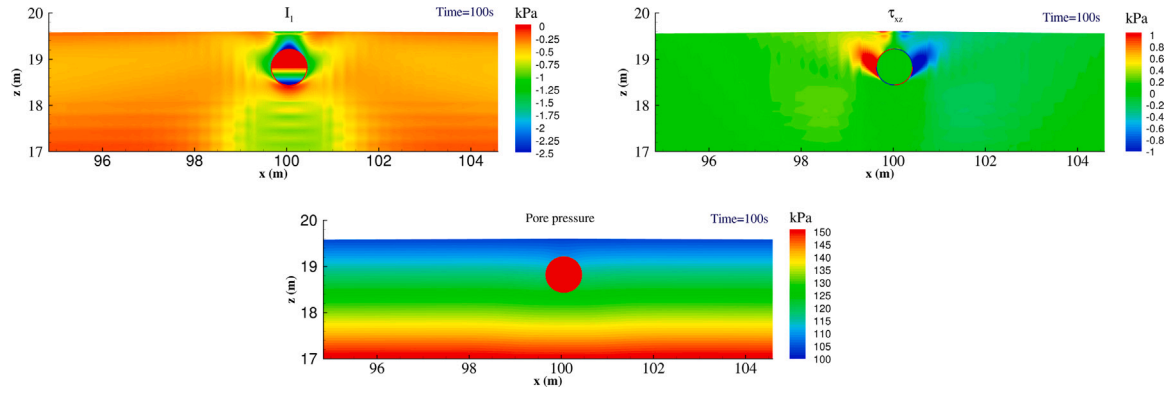

Fig. 13. Distributions of the mean effective stress I_1, shear stress τ_{xz} and pore pressure at t = 100s.

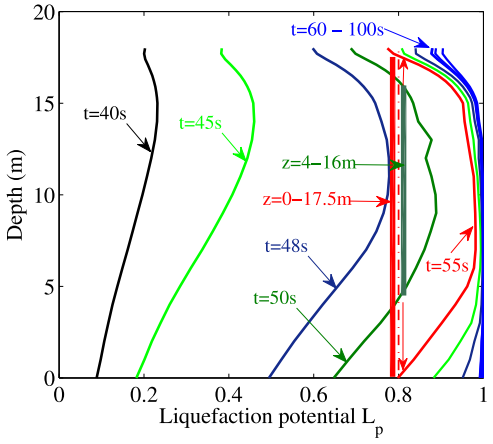

Fig. 14. Development of the liquefaction potential L_p on the symmetric line x=100 m.

in Ye and Wang (2016). Greater permeability means that pore water in the superficial layer of the seabed floor is easier to be drained out, and the pore pressure is further more difficult to build up, and is easier to be dissipated. As a result, it is quite normal that the residual liquefaction does not tend to initially occur in the superficial layer of the seabed floor under seismic waves. For hydrodynamic loads, there is a question that whether the residual liquefaction also could initially occur in the medium depth of the seabed floor? Actually, this question has been answered by Yang and Ye (2017, 2018) that the residual liquefaction can still initiate in the superficial layer of seabed floor under hydrodynamic loads, even though the permeability of loosely deposited seabed soil is great as 1.0×10^{-4} m/s. This difference is caused by the characteristics of cyclic loading. As we know, hydrodynamic loads are directly applied on the surface of seabed floor, while seismic load is input at the bottom of seabed floor.

5.5. *Effect of pipeline-gas system*

In the practice of engineering, the marine pipeline is not only used to transport crude oil, but also natural gas (density is 0.7174 kg/m^3

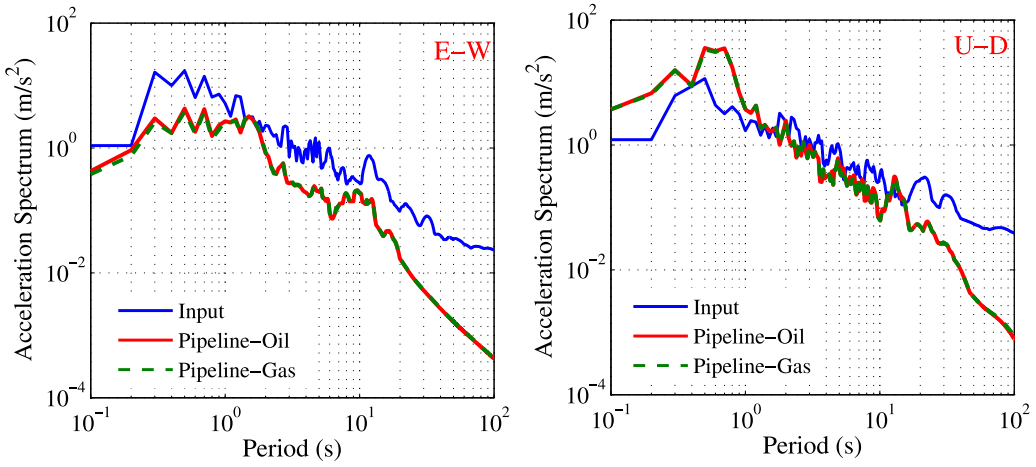

Fig. 15. Effect on the acceleration dynamics of the pipeline if natural gas is transported.

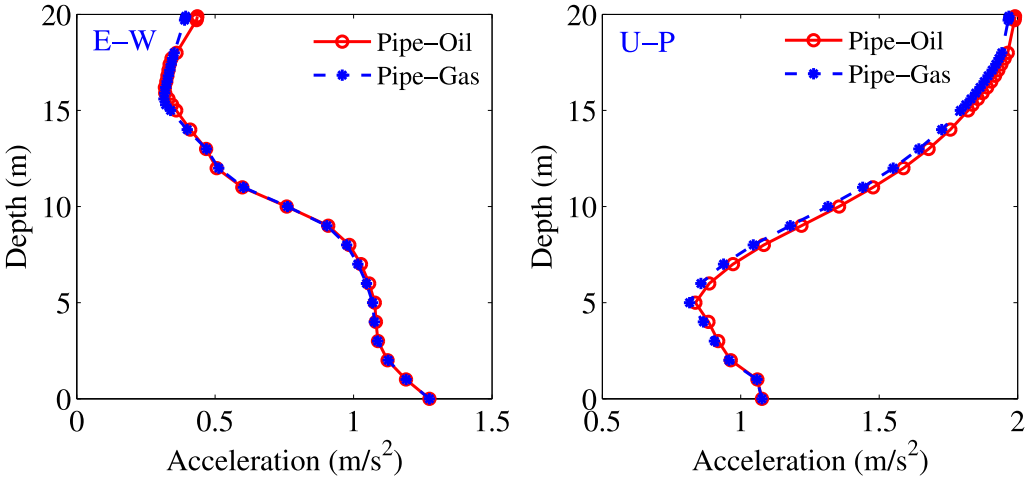

Fig. 16. Effect on the acceleration amplification in the seabed floor if natural gas is transported.

at one atmosphere). In this study, the seismic wave-induced dynamics of the pipeline-gas system buried in the same loose seabed floor is also comparatively investigated, to comprehensively explore the differences in the dynamics between the two types of pipeline system.

The acceleration spectrum of the pipeline, and the distribution of the peak acceleration on x = 100 m in the case natural gas is transported are comparatively illustrated in Fig. 15 and Fig. 16. It is found that there is basically no difference for the acceleration response of the pipeline, regardless of that crude oil or natural gas is transported by the pipeline. Meanwhile, the development of the buoyancy on the pipeline, as well as the displacement of the pipeline in the case natural gas is transported are also comparatively illustrated in Fig. 17 and Fig. 18. It is observed that there is a visible difference for the buoyancy acting on the pipeline. If natural gas is transported, the peak vertical component of the buoyancy F_z is significantly less than that if crude oil is transported. However, there is no difference for the horizontal component F_x.

It is also observed that there is no difference in the horizontal displacement of the pipeline. The effect if natural gas is transported is best reflected by the vertical displacing of the pipeline. Overall, the pipeline transporting natural gas also similarly first sinks, and then floats upward under the seismic wave attacking. However, the maximum magnitude of the floatation reaches up to 11 cm, which is nearly double that if crude oil is transported. This significant difference is definitely caused by the key factors that the gravitational weight of the pipeline-gas system is much less than that of the pipeline-oil

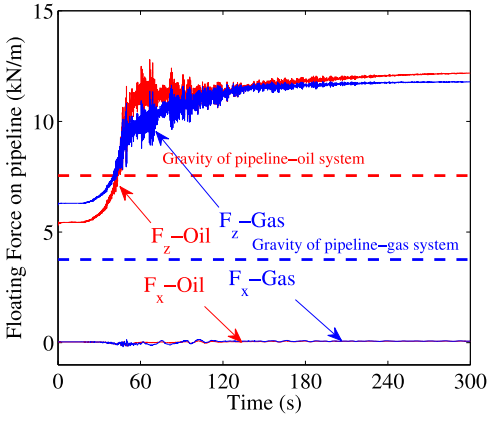

Fig. 17. Effect on the buoyancy applied on the pipeline if natural gas is transported.

system; meanwhile, there is no significant difference for the buoyancy on the pipeline resulting from the pore pressure accumulation in its surrounding soil.

The predicted liquefaction zones in the seabed floor adopting L_p when natural gas is transported are shown in Fig. 19. Compared with that demonstrated in Fig. 12, it is found that the shape of liquefaction

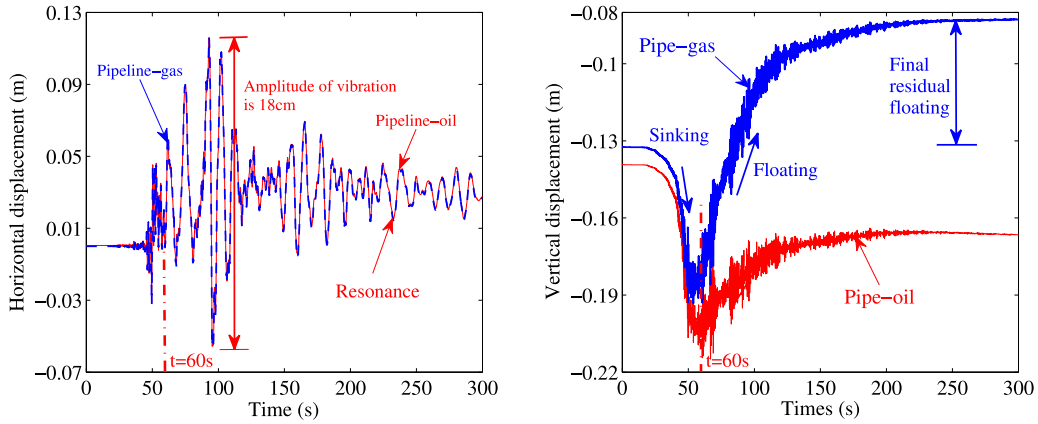

Fig. 18. Effect on the displacement of the pipeline if natural gas is transported.

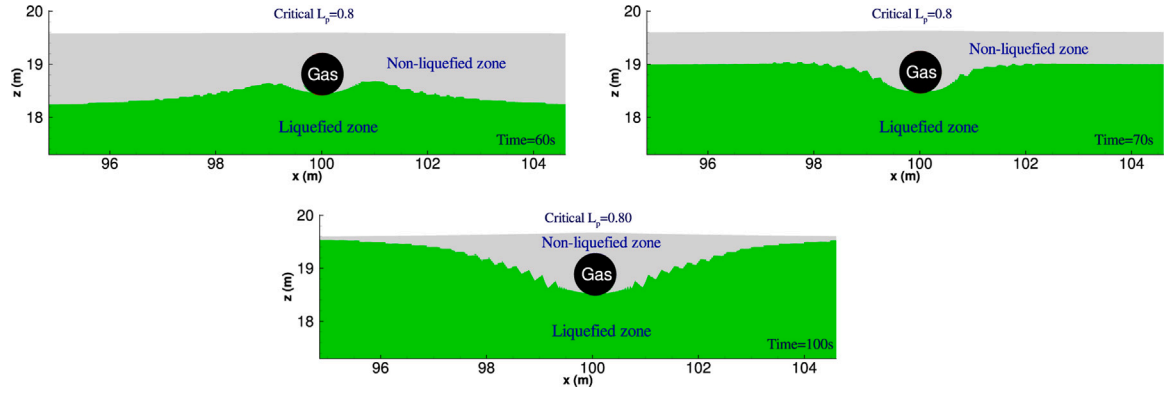

Fig. 19. Predicted liquefaction zone in the seabed floor adopting L_p for the case natural gas is transported.

zone near the pipeline in which natural gas is transported is significantly different. For the pipeline-gas system, liquefaction only occurs in a small area beneath the pipeline in its surrounding soil. The soil at the left, right-hand side of, as well as over the pipeline is not liquefied at $t = 60$ s, 70 s, and 100 s. Overall, the effect of the pipeline-gas system on the liquefaction zone near the pipeline is considerable.

5.6. Post-reconsolidation

Once the seismic wave passing, the accumulated excess pore pressure in the seabed floor will gradually dissipate accompanying the drainage out of pore water through the surface of the seabed floor. In this process, the effective stress in the seabed will increase correspondingly, and the buried pipeline will also correspondingly subside. Finally, the seabed soil will become denser, and further obtain a greater bearing capacity once the excess pore pressure is completely dissipated. The post-reconsolidation process involving the pore pressure dissipation, as well as the subsidence of the pipeline are demonstrated in Fig. 20. It is observed that the pore pressure at B firstly grows slightly, and then quickly dissipates to the hydrostatic pressure value. This is the typical "Mandel-Cryer effect", firstly revealed by Mandel (1953) and Cryer (1963). It is also observed that the pipeline indeed gradually subsides after the seismic wave finishing. The final sinking magnitude of the pipeline reaches up to about 0.45 m (crude oil is transported) and 0.37 m (natural gas is transported), respectively. This subsidence in the post-reconsolidation process is much greater than the magnitude of floatation of the pipeline, nearly reaching the magnitude order of 1 m. Also because of the greater gravitational weight of the pipeline-oil system, its subsidence is greater than that of pipeline-gas system. It should be noted that the excessive subsidence after seismic wave attacking also would be a threat to the normal service of marine pipelines. This post-reconsolidation process of the pipeline-oil/gas-seabed system is an important result for the seismic dynamic response of offshore pipelines due to the fact there is no attention has been specially paid on this issue in previous literature. It will promote us to further understand the mechanism and dynamic characteristics of marine pipelines subjected to seismic waves.

6. Conclusion

In this study, the seismic dynamic response of a shallowly buried pipeline transporting crude oil or natural gas in loosely deposited seabed floor is numerically investigated adopting the integrated model FSSI-CAS 2D. Through comprehensive analysis for the computational results, the following recognitions are obtained:

(1) There is significant pore pressure accumulation and effective stress reduction in the surrounding seabed soil of the pipeline. However, the effective stress is always away from the zero-stress state, indicating that the surrounding soil is impossible to become fully liquefied under seismic wave attacking. Soil softening must have occurred in the surrounding soil due to the accumulation of pore pressure, resulting in the partial loss of the stiffness of soil. This mechanism provides extremely favourable condition for the horizontal vibration with great amplitude, sinking, and floatation of the pipeline.

(2) There is an intensive response for the buried pipeline to the input seismic wave, and there is intensive interaction between the pipeline and its surrounding loose seabed soil. The liquefaction occurring in the surrounding soil and in the medium depth of the seabed floor plays the controlling role in the dynamics of the pipeline, for example, the horizontal responding acceleration of the pipeline will basically disappear once the soil in the medium depth of the seabed floor

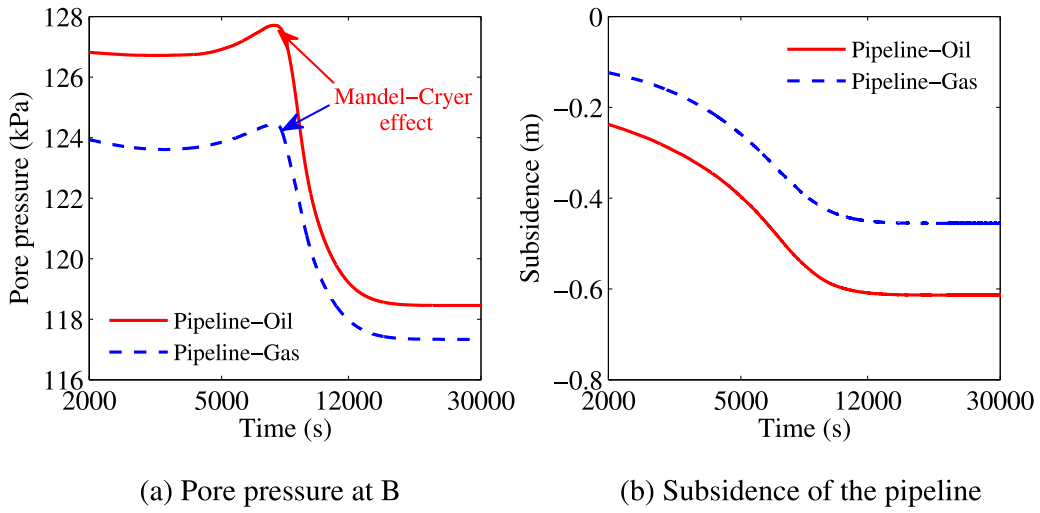

Fig. 20. Post-consolidation process of the pipeline-oil/gas-seabed system after the seismic wave attacking.

becomes fully liquefied because shear wave cannot be transmitted in the fully liquefied soil layer.

(3) Due to the significant accumulation of pore pressure, the buoyancy applied on the outer wall of the pipeline gradually grows, and finally becomes greater than the gravitational weight of the pipeline-oil/gas system. Under the continuous action of the buoyancy, the pipeline changes its motion mode from the previous sinking to subsequent floating and further leads to the apparent upheaval of the soil over the pipeline by extruding.

(4) The seismic wave-induced residual liquefaction has been evaluated by adopting two types of stress-based criteria. Overall, we tend to think that the liquefaction zone predicted by the definition of liquefaction potential L_P is more reliable for the case involved in this study. It is necessary to point out that the criteria $|I_1| \leq (I_1)_{critical}$ will also be reliable for the soil with great initial effective stress. Besides, it is found that the seismic wave-induced residual liquefaction could initiate in the medium depth of loose seabed floor, and then enlarge toward to the upper and lower seabed synchronously if the permeability of seabed soil relatively is great. Only when the permeability of seabed soil is relatively less, residual liquefaction could initiate at the superficial layer seabed floor, as that induced by hydrodynamic loads. Finally, it is observed that the seabed soil at the right, left-hand side of, as well as over the pipeline does not become liquefied due to the intensive interaction between the pipeline and its surrounding soil.

(5) Based on comparative analysis, it is found the most significant differences are reflected in the magnitude of the pipeline floatation, and in the shape of liquefaction zone in the seabed floor if natural gas is transported by the pipeline, compared with the case where crude oil is transported.

(6) After seismic wave attacking, the whole pipeline-oil/gas-seabed system gets into the post-reconsolidation process. “Mandel-Cryer effect" is observed in the process of pore pressure dissipation in the surrounding soil of the pipeline. Finally, considerable subsidence that is at the magnitude order of 1 m occurs for the pipeline in the post-reconsolidation process. It should be noted that the excessive subsidence after seismic wave attacking also would be a threat to the normal service of marine pipelines. Therefore, it is reminded to us that the subsidence of marine structures(not only marine pipeline) built on or buried in loose seabed floor in post-reconsolidation process should be evaluated in engineering practice.

(7) The computational results show that the integrated mode FSSI-CAS 2D has successfully and subtly captured a series of nonlinear physical phenomena for the intensive interaction between the buried pipeline and its loose surrounding soil, e.g., the vibration, sinking, and floating of the pipeline. It is indicated that the integrated model FSSI-CAS 2D would be a trustworthy platform to study the seismic dynamic response of marine structures.

CRediT authorship contribution statement

Jianhong Ye: Conceptualization, Methodology, Investigation, Formal analysis, Writing, Supervision, Funding acquisition. **Qianyu Lu:** Methodology, Investigation, Visualization, Formal analysis, Writing.

Declaration of competing interest

The authors declare that they have no known competing financial interests or personal relationships that could have appeared to influence the work reported in this paper.

Acknowledgement

Professor Jianhong YE are grateful to the funding support from National Natural Science Foundation of China under project 51879257.

References

Bayraktar, D., Ahmada, J., Larsena, B.E., Carstensena, S., Fuhrmana, D.R., 2016. Experimental and numerical study of wave-induced backfilling beneath submarine pipelines. Coast. Eng. 118, 63–75.

Chan, A.H.C., 1988. A Unified Finite Element Solution to Static and Dynamic Problems of Geomechanics (Ph.D. thesis). University of Wales, Swansea Wales.

Christian, T.J., Taylor, P.K., Yen, J.K.C., Erali, D.R., 1974. Large diameter underwater pipeline for nuclear plant designed against soil liquefaction. In: Proceedings of Offshore Technolgy Conference, Houston, pp. 597–606.

Cryer, C.W., 1963. A comparison of the three-dimensional consolidation theories of Biot and terzaghi. Q. J. Mech. Appl. Math. XVI (4), 401–412.

Duan, L., Liao, C.C., Jeng, D.S., Chen, L., 2017. 2D numerical study of wave and current-induced oscillatory non-cohesive soil liquefaction around a partially buried pipeline in a trench. Ocean Eng. 135, 39–51.

Dunn, S.L., Vun, P.L., Chan, A.H.C., Damgaard, J.S., 2006. Numerical modeling of wave-induced liquefaction around pipelines. J. Waterw. Port Coast. Ocean Eng. 132 (4), 276–288.

Ecemis, N., Valizadeh, H., Karaman, M., 2021. Sand-granulated rubber mixture to prevent liquefaction-induced uplift of buried pipes: a shaking table study. Bull. Earthq. Eng. 19, 2817–2838.

Fredsøe, J., 2016. Pipeline–seabed interaction. J. Waterway, Port, Coastal, and Ocean Engineering, ASCE 142 (6), 03116002.

Gao, F.P., Wu, Y.X., 2006. Non-linear wave-induced transient response of soil around a trenched pipeline. Ocean Eng. 33, 311–330.

He, K.P., Huang, T.K., Ye, J.H., 2018. Stability analysis of a composite breakwater at yantai port, China: An application of FSSI-CAS-2D. Ocean Eng. 168, 95–107.

Herbich, J.B., Schiller, R.E., Dunlap, W.A., Watanabe, R.K., 1984. Seafloor Scour, Design Guidelines for Ocean-Founded Structures. Marcel Dekker, New York.

Jeng, D.-S., Ye, J.H., Zhang, J.-S., Liu, P.-F., 2013. An integrated model for the wave-induced seabed response around marine structures: Model, verifications and applications. Coast. Eng. 72 (1), 1–19.
Kiziloz, B., Cevik, E., Yuksel, Y., 2013. Scour below submarine pipelines under irregular wave attack. Coast. Eng. 79, 1–8.
Larsen, B.E., Fuhrman, D.R., Sumer, B.M., 2016. Simulation of wave-plus-current scour beneath submarine pipelines. J. Waterw. Port Coast. Ocean Eng. 142 (5), 04016003.
Ling, H.I., Sun, L.X., Liu, H.B., Mohri, Y., Kawabata, T., 2008. Finite element analysis of pipe buried in saturated soil deposit subject to earthquake loading. J. Earthq. Tsunami 2 (1), 1–17.
Luan, M., Qu, P., Jeng, D.S., Guo, Y., Yang, Q., 2008. Dynamic response of a porous seabed-pipeline interaction under wave loading: Soil-pipeline contact effects and inertial effects. Comput. Geotech. 35, 173–186.
Luan, M.T., Zhang, X.L., Yang, Q., Guo, Y., 2009. Numerical analysis of liquefaction of porous seabed around pipeline fixed in space under seismic loading. Soil Dyn. Earthq. Eng. 29, 855–864.
Mandel, J., 1953. Consolidation des sols (tude math matique). Géotechnique 3, 287–299.
Miyamoto, J., Sassa, S., Sekiguchi, H., 2004. Progressive solidification of a liquefied sand layer during continued wave loading. Géotechnique 54 (10), 617–629.
Miyamoto, J., Sassa, S., Tsurugasaki, K., Sumida, H., 2020. Wave-induced liquefaction and floatation of a pipeline in a drum centrifuge. J. Waterw. Port Coas. Ocean Eng., ASCE 146 (2), 04019039.
Pastor, M., Chan, A.H.C., Mira, P., Manzanal, D., Fernandez, M.J.A., Blanc, T., 2011. Computational geomechanics: The heritage of Olek Zienkiewicz. Internat. J. Numer. Methods Engrg. 87 (1–5), 457–489.
Saeedzadeh, R., Hataf, N., 2011. Uplift response of buried pipelines in saturated sand deposit under earthquake loading. Soil Dyn. Earthq. Eng. 31, 1378–1384.
Sassa, S., Sekiguchi, H., 2001. Analysis of wave-induced liquefaction of sand beds. GÉotechnique 51 (2), 115–126.
Summer, B.M., Truelsen, C., Fredsoe, J., 2006. Liquefaction around pipeline under waves. J. Waterw. Port Coast. Ocean Eng. 132 (4), 266–275.
Teh, T.C., Palmer, A.C., Damgaard, J.S., 2003. Experimental study of marine pipelines on unstable and liquefied seabed. Coast. Eng. 50 (1–2), 1–17.
Wu, J., Kammaerer, A.M., Riemer, M.F., Seed, R.B., Pestana, J.M., 2004. Laboratory study of liquefaction triggering criteria. In: Proceedings of 13th World Conference on Earthquake Engineering, Vancouver, British Columbia, Canada, Paper No. 2580.
Yang, G.X., Ye, J.H., 2017. Wave & current-induced progressive liquefaction in loosely deposited seabed. Ocean Eng. 142, 303–314.
Yang, G.X., Ye, J.H., 2018. Nonlinear standing wave-induced liquefaction in loosely deposited seabed. Bull. Eng. Geol. Environ. 77 (1), 205–223.
Ye, J.H., He, K.P., 2021. Dynamics of a pipeline buried in loosely deposited seabed to nonlinear wave & current. Ocean Eng. 232, 109127.
Ye, J.H., Jeng, D.-S., Liu, P.L.-F., Chan, A.H.C., Wang, R., Zhu, C.-Q., 2014. Breaking wave-induced response of composite breakwater and liquefaction of seabed foundation. Coast. Eng. 85, 72–86.
Ye, J.H., Jeng, D.-S., Wang, R., Zhu, C.-Q., 2013a. Numerical study of the stability of breakwater built on sloped porous seabed under tsunami loading. Appl. Math. Model. 37, 9575–9590.
Ye, J.H., Jeng, D.-S., Wang, R., Zhu, C.-Q., 2013b. Validation of a 2D semi-coupled numerical model for fluid-structures-seabed interaction. J. Fluids Struct. 42, 333–357.
Ye, J.H., Wang, G., 2015. Seismic dynamics of offshore breakwater on liquefiable seabed foundation. Soil Dyn. Earthq. Eng. 76, 86–99.
Ye, J.H., Wang, G., 2016. Numerical simulation of the seismic liquefaction mechanism in an offshore loosely deposited seabed. Bull. Eng. Geol. Environ. 75 (3), 1183–1197.
Zhang, X.L., Han, Y., 2013. Numerical analysis of seismic dynamic response of saturated porous seabed around a buried pipeline. Mar. Georesources Geotechnol. 31 (3), 254–270.
Zhang, X.L., Jeng, D.S., Luan, M.T., 2011. Dynamic response of a porous seabed around pipeline under three-dimensional wave loading. Soil Dyn. Earthq. Eng. 31, 785–791.
Zhang, Y., Ye, J.H., He, K.P., Chen, S.G., 2019. Seismic dynamics of pipeline buried in dense seabed foundation. J. Mari. Sci. Eng. 7 (6), 190.
Zhao, K., Xiong, H., Chen, G.X., Zhao, D., Chena, W., Du, X., 2018. Wave-induced dynamics of marine pipelines in liquefiable seabed. Coast. Eng. 140, 100–113.
Zhou, X.L., Zhang, J., Guo, J.K., Wang, J.H., Jeng, D.S., 2015. Cnoidal wave induced seabed response around a buried pipeline. Ocean Eng. 101, 118–130.
Zienkiewicz, O.C., Chan, A.H.C., Pastor, M., Schrefler, B.A., Shiomi, T., 1999. Computational Geomechanics with Special Reference to Earthquake Engineering. John Wiley and Sons, England.
Zienkiewicz, O.C., Mroz, Z., 1984. Generalized plasticity formulation and applications to geomechanics. In: Mechanics of Engineering Materials. John, Chichester.